Article

Rapid and Amplification-free Nucleic Acid Detection with DNA Substrate-Mediated Autocatalysis of CRISPR/Cas12a

Zhongqi Zhou,[○] Cia-Hin Lau,[○] Jianchao Wang,[○] Rui Guo, Sheng Tong, Jiaqi Li, Wenjiao Dong, Zhihao Huang, Tao Wang, Xiaojun Huang, Ziqing Yu, Chiju Wei, Gang Chen,* Hongman Xue,* and Haibao Zhu*

Read Online

ACCESS | Metrics & More | Article Recommendations | SI Supporting Information

ABSTRACT: To enable rapid and accurate point-of-care DNA detection, we have developed a single-step, amplification-free nucleic acid detection platform, a DNA substrate-mediated autocatalysis of CRISPR/Cas12a (DSAC). DSAC makes use of the trans-cleavage activity of Cas12a and target template-activated DNA substrate for dual signal amplifications. DSAC employs two distinct DNA substrate types: one that enhances signal amplification and the other that negatively modulates fluorescent signals. The positive inducer utilizes nicked- or loop-based DNA substrates to activate CRISPR/Cas12a, initiating trans-cleavage activity in a positive feedback loop, ultimately amplifying the fluorescent signals. The negative modulator, which involves competitor-based DNA substrates, competes with the probes for

trans-cleaving, resulting in a signal decline in the presence of target DNA. These DNA substrate-based DSAC systems were adapted to fluorescence-based and paper-based lateral flow strip detection platforms. Our DSAC system accurately detected African swine fever virus (ASFV) in swine's blood samples at femtomolar sensitivity within 20 min. In contrast to the existing amplification-free CRISPR/Dx platforms, DSAC offers a cost-effective and straightforward detection method, requiring only the addition of a rationally designed DNA oligonucleotide. Notably, a common ASFV sequence-encoded DNA substrate can be directly applied to detect human nucleic acids through a dual crRNA targeting system. Consequently, our single-step DSAC system presents an alternative point-of-care diagnostic tool for the sensitive, accurate, and timely diagnosis of viral infections with potential applicability to human disease detection.
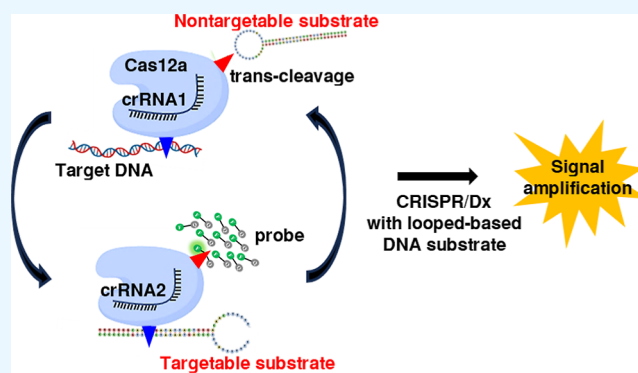
INTRODUCTION

CRISPR-based diagnostics, CRISPR/Dx, has become an increasingly popular molecular diagnostic tool owing to its attractive features, including enabling visual readout, portable diagnostics, and home self-testing, as no costly equipment and trained personnel is required, allowing for the detection of viruses directly from body fluids, sequence-targeted single-base specificity, and quick and reliable diagnosis of viral disease without the need for complex lab protocols.[1,2] CRISPR/Dx employs the single-stranded nucleic acid trans-cleavage activities of either Cas12[3,4] or Cas13.[5,6] This inherent signal amplification capability allows CRISPR/Dx to detect target nucleic acids with minimal copy numbers.

Despite the great potential of CRISPR/Dx in pathogen detection, preamplification of the template through isothermal amplification or polymerase chain reaction (PCR) is often required for the sensitive detection of low-abundance nucleic acids.[7,8] This additional preamplification step led to long detection time, complex operation, susceptibility to impurities in a complex biofluid, sequence bias amplification of the

template, and false-positive results owing to amplification errors or carryover contamination.[9] A PCR-based preamplification step also requires purified nucleic acid, accurate temperature control, and a bulky and sophisticated thermal cycling instrument. This renders their use in resource-limited and point-of-care settings. Although isothermal amplification operates at constant low temperatures using miniature devices, it requires multiple enzymes and complex primers.

To enable direct detection of target nucleic acids without preamplification, various amplification-free CRISPR/Dx systems have been developed to enhance signal detection in recent years.[9−16] CRISPR/Dx has been coupled to fluorimeters, spectrometers, microfluidic devices, field-effect transis-
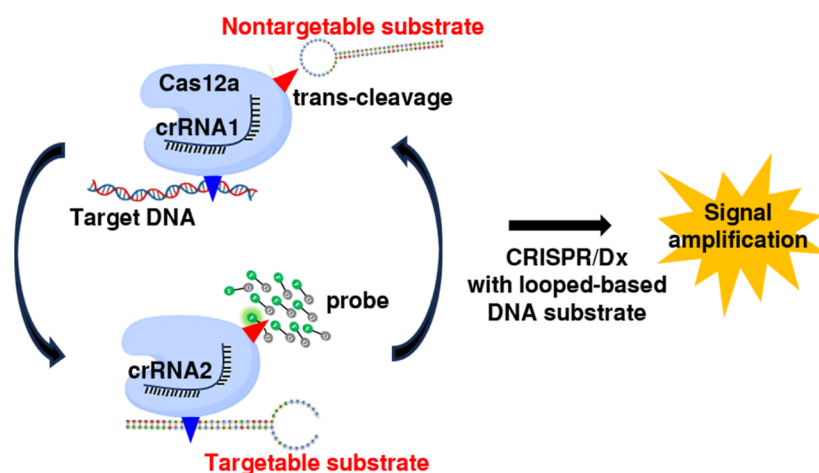
Figure 1. Detection principle of a loop-based DNA substrate-mediated DSAC system. The addition of loop-based DNA substrates to the CRISPR/Cas12a complex results in a cascade amplification effect. crRNA2 is used to target the ASFV DNA sequence on the DNA substrate, while crRNA1 is used to target the desired DNA sequences such as human genomic DNA.

tors, or amperometric biosensors to realize target amplification-free detection.[9,11] In general, sensitivity was increased by improving the trans-cleavage capability and signal amplification. Whereas the detection sensitivity of these amplification-free CRISPR/Dx systems could be comparable to that of amplification-based methods, their detection relies on expensive devices and complicated procedures and is high in cost due to the use of multiple or special materials.

To enable rapid and accurate point-of-care DNA detection, here we have developed an amplification-free CRISPR-Dx system, termed a DNA substrate-mediated autocatalysis of CRISPR/Cas12a (DSAC). DSAC utilizes target DNA-activated Cas12a to convert exogenous DNA substrates into targetable artificial templates in response to the trans-cleavage activity of active Cas12a. Subsequently, artificial templates activate the remaining inactive Cas12a. These activated Cas12a each have their trans-cleavage activities to cleave and turn the DNA substrates into targetable artificial templates. As the number of targetable artificial templates increases, the number of active Cas12a and trans-cleavage activities also increases to cleave the reporter, thereby amplifying the fluorescent signals. In addition, we unexpectedly discovered a substrate DNA that negatively modulates the fluorescence signal. In this proof-of-concept study, the DSAC system was used to detect unamplified nucleic acids. The DSAC system was applied in fluorescence-based and paper-based lateral flow strip detection platforms. We validated the practical application of the proposed DSAC system using undiluted blood samples from the swine. Finally, we demonstrate the feasibility of using the DSAC system in detecting human DNA. Because of its cost-effective, simple procedures, rapid detection, and high selectivity, our DSAC system can be potentially used for site inspection and point-of-care detection of viral infections and human disease.

RESULTS

Screening of DNA Substrates for the DSAC System. As illustrated in Figure 1, DNA substrates consist of two components: one part serves as a target recognition sequence for crRNA2, while the other part consists of a unique structure (Figure 1, close loop; Figure S1, flap fragment) that hinders the binding of the Cas12a/crRNA2 complex to the substrate

DNA. Upon the introduction of target DNA, Cas12a/crRNA1 recognizes the target DNA, activating the trans-cleavage activity of Cas12a. Active Cas12a not only leads to collateral cleavage of ssDNA probes in the reaction mixture but also cleaves T-rich ssDNA on the substrate DNA. As a consequence, the conformation of the DNA substrate is altered, enabling Cas12a/crRNA2 access and binding to the DNA substrate. The binding of Cas12a/crRNA2 to the DNA substrate activates more Cas12a with trans-cleavage activities, resulting in collateral cleavage of additional probes and T-rich ssDNA on the substrate DNA. Subsequently, each target DNA molecule is converted into cascade reactions, thereby exponentially amplifying the fluorescence signals. In the absence of a target DNA template, the DNA substrate remains in a nontargetable form due to a lack of trans-cleavage activity of Cas12a. As a consequence, a weak fluorescent signal was generated. Likewise, with the mere presence of a limited copy of target DNA template (absence of DNA substrates), no fluorescent signal could be detected. It is to be noted that crRNA2 was used to target the African swine fever virus (ASFV) DNA sequence on the DNA substrate, while crRNA1 was programmed to target the desired DNA sequence such as human genomic DNA. We have screened and confirmed the high functionality of T8-crRNA2; therefore, the DNA sequence targeting by T8-crRNA2 was used to assemble all DNA substrates (Figure S2). Conversely, a minimum of 109 nM of plasmid templates was needed for reliable fluorescent signal detection when employing the classical CRISPR/Cas12a system (without adding a DNA substrate).

DNA substrates that were tested in this study were classified into a nicked-based DNA substrate (Figure S3A, Tables S1 and S2) and loop-based DNA substrate (Figure S3B, Tables S1 and S2). The native conformation of a nicked-based DNA substrate is nontargetable due to the presence of the flap fragment at the center of the crRNA target site. The flap fragment was introduced to one of the strands of the DNA substrate, in which this DNA strand is complementary to the crRNA target sequence. The neck of the flap fragment consists of a stretch of thymine nucleotides to enhance trans-cleavage activity, while the terminus was designed with dsDNA to block Cas12a/crRNA2 recognition and minimize background signals. In the presence of target DNA, a nicked-based DNA substrate is converted into a targetable template through the removal of
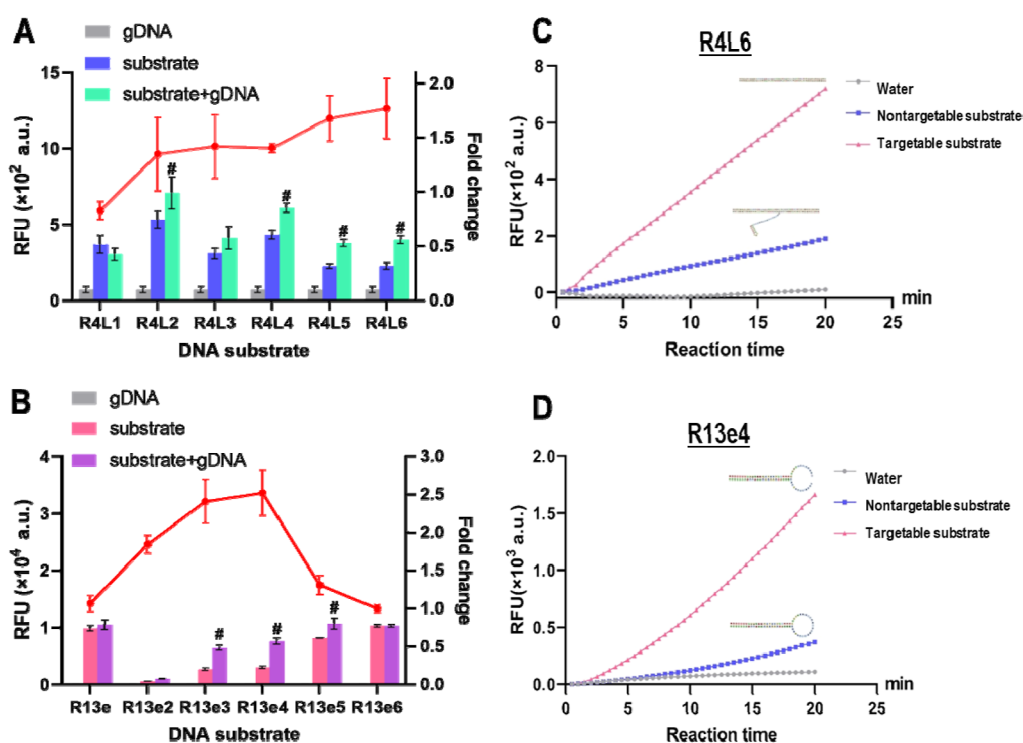
Figure 2. Functional screening of DNA substrates. Fluorescent signals (RFU, left) generated by various (A) nicked-based and (B) loop-based DNA substrates. Fold change (right) is the relative fluorescence intensity of reactions in the presence and absence of target DNA. All experiments were performed in triplicate. (C) Comparison of nicked dsDNA and nicked-based DNA substrate bearing a flap fragment. Nicked dsDNA was formed by annealing of three ssDNAs with a nick in one of the DNA strands. Fluorescent analysis shows that nicked dsDNA can be recognized by a Cas12a–crRNA complex, thereby serving as a template to activate Cas12a. Fluorescent data also confirm the ability of a flap fragment to block the recognition and binding of CRISPR/Cas12a to the R4L6 DNA substrate; therefore, the background signal is low. (D) Comparison of linear dsDNA and loop-based DNA substrates in activating Cas12a. Linear dsDNA was formed by annealing of two ssDNAs that are complementary to each other except at the 3′ end. Unmatched 3′ end has similar sequences to the loop in the DNA loop. The sequences in the loop contain a small part of the protospacer crRNA and the PAM sequences. Fluorescent analysis shows that Cas12a has better recognition in linear dsDNA than the DNA loop and therefore locates part of the protospacer crRNA, and the PAM sequences in the loop can block the Cas12a recognition and binding. P values less than 0.05 were considered statistically significant with *$p < 0.05$ and #$p < 0.01$.

the flag fragment catalyzed by the trans-cleavage activity of active Cas12a. As the fluorescent signals of the nicked-based DNA substrate bearing the flap fragment were substantially lower than those of the nicked DNA substrate without the flap fragment, we confirm that the insertion of the flap fragment was able to block the recognition and binding of Cas12a/crRNA2. To screen the best structure of the flap fragment, we have designed nicked-based DNA substrates with different conformations of the flap fragment. We evaluated their performance relative to the negative control (absence of target DNA) using a fluorescent detection approach. The fold change (relative fluorescent signal) was formulated as follows: DNA substrate with a target DNA/DNA substrate without target DNA. Higher fold change indicates a better discrimination capability when the target DNA template is present. When testing DNA substrates with various flap fragments, we identified R4L6 as the most promising nicked-based DNA substrate owing to the highest fold change value (Figure 2A). However, the efficiency of cascade signal amplification with the R4L6 DNA substrate remains low.

Therefore, we proceeded to design another conformation of DNA substrates such as loop-based DNA substrates (Figure S3B, Tables S1 and S2). The original conformation of a loop-based DNA substrate is nontargetable due to the steric hindrance by the loop structure. In this example, the target recognition sequence of crRNA2 is 23 bp. To minimize

background signals and maximize the sensitivity of detection, the DNA substrate was designed to locate the 19 bp crRNA2-targeting sequence in the dsDNA stem structure and 5 bp in the loop. The loop was designed to contain a stretch of thymine nucleotides to enhance trans-cleavage activities. In the presence of target DNA, active Cas12a/crRNA1 trans-cleaved the loop and linearized the DNA substrate. The targetable linearized DNA substrate then served as a substrate for activating other Cas12a/crRNA2. The cascade reactions and autocatalysis led to collateral cleavage of the excess probes, thereby amplifying the fluorescent signals for detection. To enhance the specificity and minimize the background fluorescent signals, a substitution mutation was subsequently introduced to the loop-based DNA substrate at a different distance from the closed loop (Figure S3B). We found that single-nucleotide mismatches did not impair the capacity of a potent crRNA2 to recognize the DNA substrate despite a significant decrease in the detection sensitivity and fluorescent intensity (Figure 2B). However, we took advantage of this tolerance to improve the signal-to-noise ratio and discrimination capability of our loop-based DNA substrate DSAC system. For example, the DNA substrate with a single-base mismatch provides a significantly higher signal-to-noise ratio and discrimination capability than the unmutated DNA substrate. Among these mutated DNA substrates, we identified that R13e4 provides the highest signal-to-noise ratio and
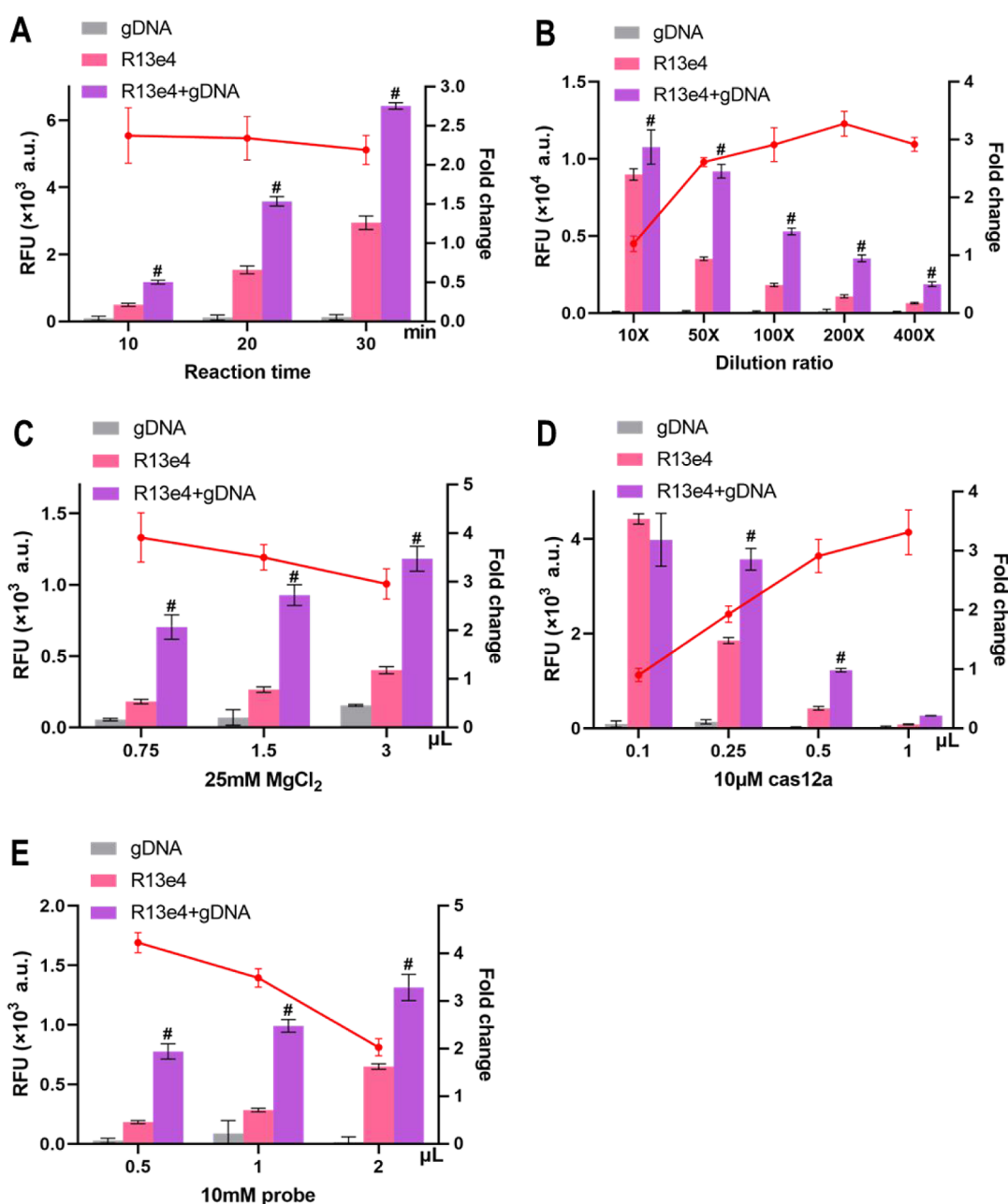
Figure 3. Optimization of the R13e4-based DSAC system. To maximize the detection sensitivity of CRISPR/Cas12 in the DSAC system, several parameters were optimized, including the (A) reaction time of CRISPR/Cas12a and the concentrations of the (B) R13e4 DNA substrate, (C) MgCl$_2$, (D) Cas12a, and (E) probe. Fluorescent signals (RFU, left) are generated under different experimental conditions. Fold change (right) is the relative fluorescence intensity of reactions in the presence and absence of a target DNA. All experiments were performed in triplicate. P values less than 0.05 were considered statistically significant with *$p < 0.05$ and #$p < 0.01$.

discrimination capability. To verify the proposed molecular mechanisms and detection principles, we directly compared the signal enhancement effects of the R4L6 nicked-based DNA substrate (Figure 2C) and the R13e4 loop-based DNA substrate (Figure 2D) at various conformations without adding Cas12a/crRNA1. These conformations mimic the structure of DNA substrates before and after trans-cleavage by active Cas12a/crRNA1.

Optimization of the R13e4-Based DSAC System. As R13e4 was the most potent loop-based DNA substrate to enhance signal amplification, we selected a R13e4-based DSAC system for detection. To maximize the detection sensitivity of the R13e4-based DSAC system, several parameters, including

the reaction time of CRISPR/Cas12a, and concentrations of the R13e4 DNA substrate, MgCl$_2$, Cas12a, and probe were evaluated (Figure 3). We tested three reaction times (10, 20, and 30 min) (Figure 3A) and found that the relative fluorescent signals reached a plateau within 10 min. However, the fluorescent intensity was low at a reaction time of 10 min. Therefore, 20 min was selected as the optimal reaction time because the fluorescent intensity was substantially higher and less variable between replicates.

To have sufficient fluorescent intensity at minimal background signals, the concentration of the DNA substrate was diluted from 10 to 400 times for testing. 200× dilution of 3 μM stock of annealed R13e4 DNA substrates gave the highest
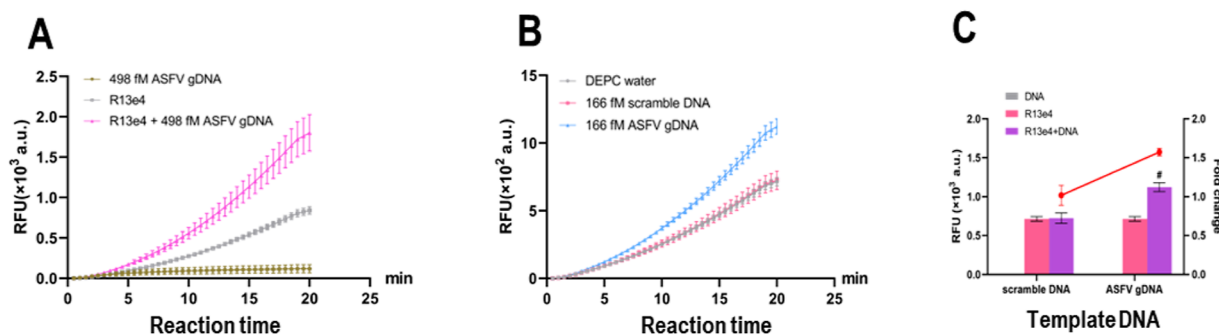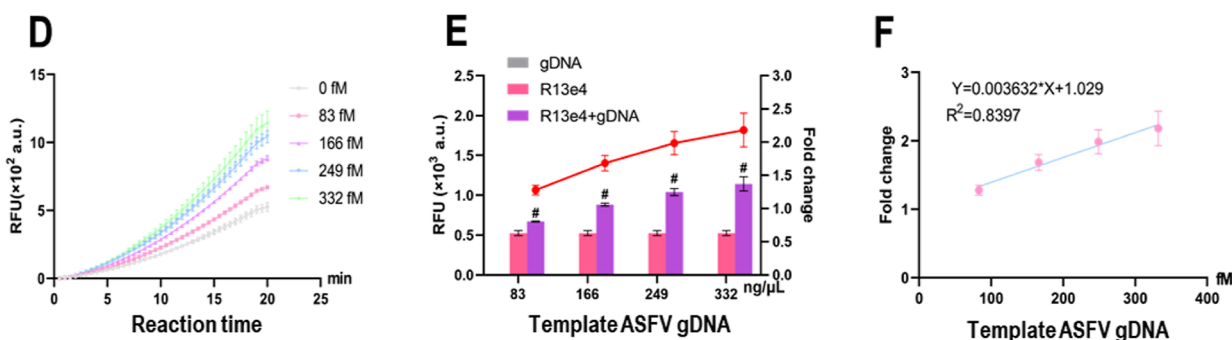
Figure 4. Specificity and sensitivity of the R13e4-based DSAC system. (A) R13e4 DNA substrate enhances the detection of ASFV target DNA. (B) R13e4 DNA substrate specifically detects ASFV target DNA. (C) Fluorescent signals in the presence of scrambled DNA and ASFV gDNA. (D) Dose-dependent effects of ASFV genomic DNA on R13e4-enhanced DSAC detection. (E) Using R13e4 as a DNA substrate, our DSAC system is able to distinguish target gDNA from scramble DNA at the LOD of 166fM ASFV genomic DNA. (F) Proportional of ASFV genomic DNA amount to fold change of fluorescent signals. All experiments were performed in triplicate. P values less than 0.05 were considered statistically significant with $*p < 0.05$ and $\#p < 0.01$.

relative fluorescent signals when compared to negative control (without ASFV genomic DNA) (Figure 3B). A lower dilution factor leads to a higher fluorescent background, while a dilution factor above 200× results in low fluorescent intensity. To ensure high discrimination capability and strong fluorescent signal in the presence of target DNA, a 200× dilution factor was selected along the experiments. As shown in Figure 3C, with the increase of the $MgCl_2$ concentration, the relative fluorescent signals decreased, but the difference was not significant. As 1.5 μL of 25 mM $MgCl_2$ gave the highest experimental consistency with high relative fluorescent signals, this concentration of $MgCl_2$ was selected for the downstream experiments. Mg^{2+} ions are required for stabilizing PAM-distal DNA unwound conformation and promoting the binding and cleavage of the target strand.[7,8]

Next, we optimized the Cas12a concentration of our DSAC system. As the dosage of Cas12a enzymes increases, the relative fluorescent signals increase and reach the plateau at 0.5 μL of 10 μM Cas12a (Figure 3D). The availability of more active Cas12a generates more targetable DNA substrates and hence a higher number of trans-cleavage activities to cleave reporter. Eventually, this positive feedback circuit leads to signal amplification. Since the relative fluorescent signal was statistically no different between 0.5 and 1.0 μL, 0.5 μL of Cas12a was selected to minimize the cost of detection. Finally, we selected 1 μL instead of 0.5 μL of 10 mM probes for the downstream experiments (Figure 3E), because a 1 μL probe

generated stronger fluorescent signals despite a slightly low fold change. A higher concentration of fluorescent probes decreased the relative fluorescent signals owing to the competition between the probes and DNA substrates for trans-cleavage.

Specificity of the DSAC System in Detecting Purified ASFV Genomic DNA. After optimizing our R13e4-based DSAC system, we first tested the specificity in detecting purified ASFV genomic DNA. We first compare our DSAC system with the traditional CRISPR/Cas12a method (Figure 4A). The result showed that in the absence of the R13e4 DNA substrate, unamplified ASFV genomic DNA was not detectable using the traditional CRISPR/Cas12a system. Likewise, the addition of the R13e4 DNA substrate without the target DNA (ASFV genomic DNA) would lead to low fluorescent signal generation. In the presence of both the target DNA and R13e4 DNA substrate, a substantial increase in fluorescent signals was observed. This indicates that our DSAC system can improve the discrimination capability and provide better limit of detection (LOD) than the traditional CRISPR/Cas12a system. The addition of scramble DNA would not increase the number of fluorescent signals, thereby confirming the specificity of our DSAC system in detecting ASFV genomic DNA (Figure 4B,C). To achieve a confidence level of at least 99.7% in detection, the relative fluorescent threshold was set at mean + 3 SD = 1.018 + 3 × 0.115 = 1.363 ≈ 1.5.[17] Using the R13e4-based DSAC system, the sample was regarded ASFV-positive if
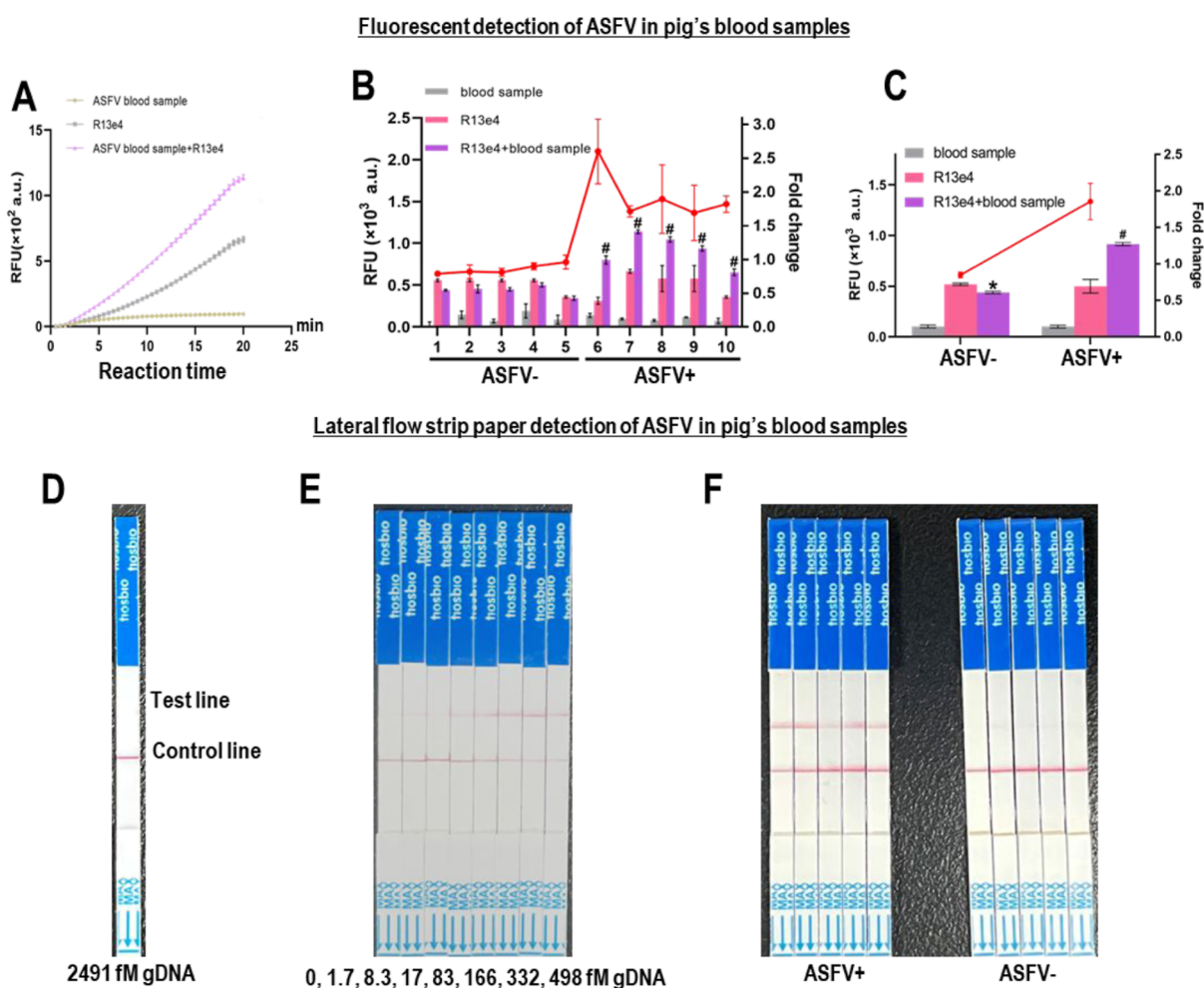
Figure 5. Fluorescent detection of ASFV in swine blood samples. (A) DNA substrate enhanced ASFV detection in swine blood samples. (B) Relative fluorescent intensity. (C) Mean relative fluorescent intensity of five samples in each group. Fold change is the relative fluorescence intensity of reactions in ASFV-positive blood samples and ASFV-negative blood samples. Lateral flow strip paper detection of ASFV in swine's blood samples at (D) high load of ASFV genomic DNA without an added DNA substrate and (E) minimal load of ASFV genomic DNA but with an added DNA substrate. (F) DSAC system is able to distinguish blood samples with ASFV ($n = 5$) and without ASFV ($n = 5$). All experiments were performed in three replications. P values less than 0.05 were considered statistically significant with $*p < 0.05$ and $\#p < 0.01$.

the fluorescent signal relative to the negative control (DNA substrate without target DNA) exceeded 1.5. Although our DSAC system was tolerant to the target DNA template with single-base mismatches, it was capable of discriminate multiple mismatches (3−4 mismatches) (Figure S4). As the effect of the target DNA template with multiple mismatches was similar to scramble control (nonrelevant sequence), scramble control was used as a negative control along the experiments.

LOD of the DSAC System in Detecting Purified ASFV Genomic DNA. Next, we determined the dose-dependent effects of ASFV genomic DNA on fluorescent intensity in the DSAC system (Figure 4D). As the amount of target DNA added increases, the fluorescent intensity also increases. At 20 min of reaction time, despite some fluorescent background induced by the R13e4 DNA substrate, our DSAC system was able to distinguish target gDNA from scramble DNA at LOD of 166 fM ASFV genomic DNA (Figure 4E). The threshold was set at a 1.5-fold change. As expected, the amount of ASFV genomic DNA added was directly proportional to the relative fluorescence signals (Figure 4F). The copy number of ASFV genomic DNA was validated with digital PCR (Figure S5).

Detection of ASFV Infection in Blood Samples from the Swine using Our DSAC System. Next, we validated the practical application of the R13e4-based DSAC system using undiluted blood samples from the swine. The presence of ASFV infections in these blood samples has been validated with the qPCR approach (Figure S6). In fluorescence-based detection platforms, the DSAC system directly detected ASFV in blood samples after the addition of a sample release agent, whereas the traditional CRISPR/Dx approach was unable to detect it (Figure 5A). Next, we used our DSAC system to detect 10 blood samples, including five blood samples with ASFV infections and five blood samples without ASFV infections. Similar to purified ASFV genomic DNA above, the relative fluorescent threshold was defined as 1.5. We found that the relative fluorescent signal was consistently >1 5 for blood samples with ASFV infections, whereas the relative fluorescent signal was less than 1.5 for blood samples without ASFV infections (Figure 5B,C). Therefore, our DSAC system can accurately and sensitively detect ASFV infection in blood samples from the swine.

Application of the DSAC System in a Lateral Flow Strip Paper Detection Platform. To dismiss the back-
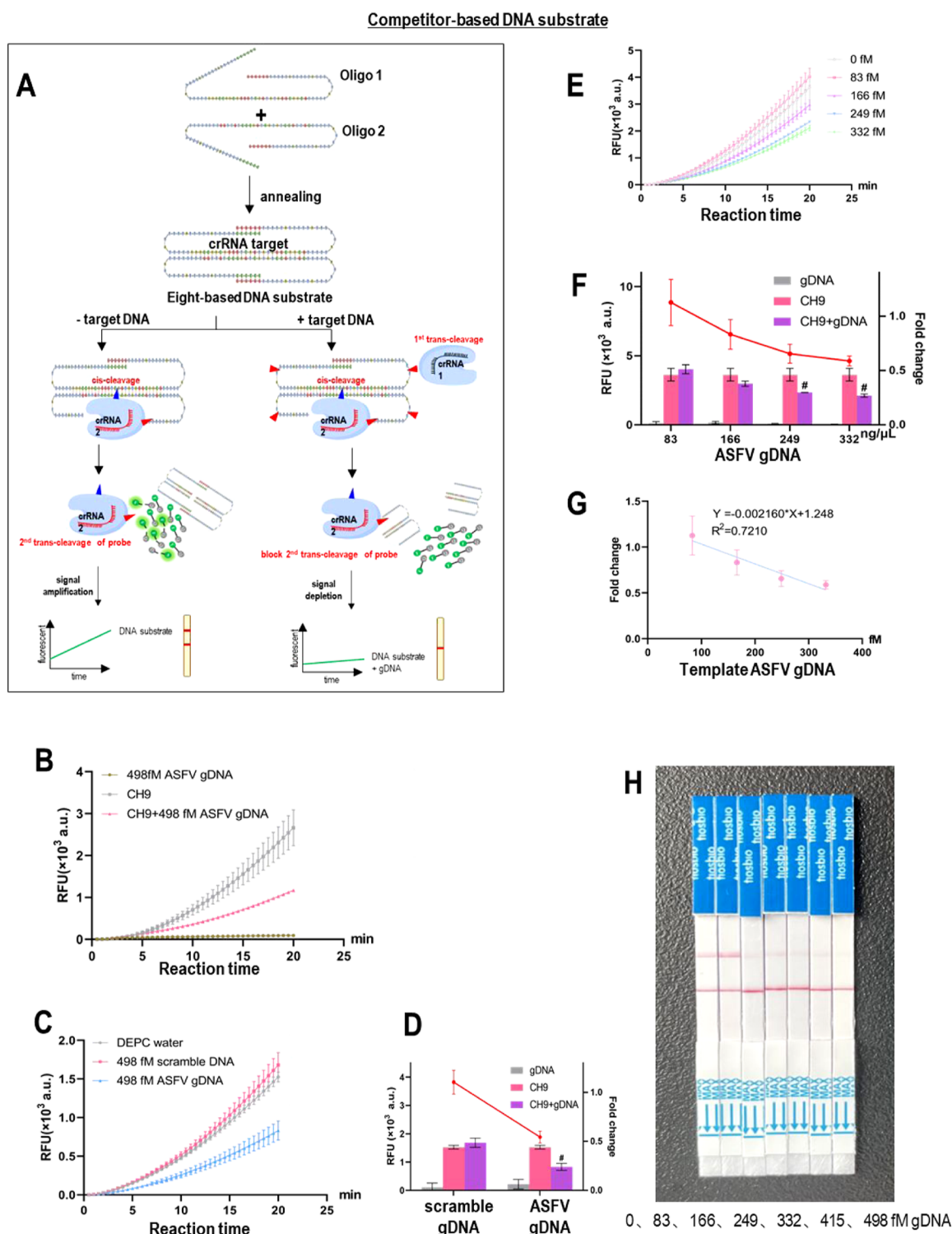
Figure 6. Target DNA detection with a competitor-based DNA substrate. (A) Scheme for a competitor-based DNA substrate DSAC system. Without the target DNA, there is no trans-cleavage activity to cleave the T-rich loop. Only Cas12a with crRNA 2 (targeting DNA substrate) is activated to bind and cleave the dsDNA on the DNA substrate. In the presence of a target DNA, Cas12a with crRNA 1 (targeting genomic DNA) is activated to bind and cleave the T-rich loops. Cas12a with crRNA 2 is also activated to bind and cleave dsDNA on the DNA substrate. The resulting two DNA fragments will compete/block the probes from trans-cleavage activity. (B) Competitor-based DNA substrates enable the detection of ASFV genomic DNA. (C,D) High specificity in detection with a competitor-based DNA substrate DSAC system. (E−G) LOD of the competitor-based DNA substrate DSAC system. (H) Application of a competitor-based DNA substrate DSAC system in lateral flow strip paper detection. All experiments were performed in triplicate. P values less than 0.05 were considered statistically significant with *$p < 0.05$ and #$p < 0.01$.

ground fluorescent signals generated by the R13e4 DNA substrate, we applied our DSAC system to a paper-based lateral flow strip detection platform. As this paper-based detection platform is not as sensitive as the fluorescent-based detection approach, it enabled the detection of positive samples without background signals, as seen in the latter approach. However,

the use of lateral flow strip paper allows for quick and home-testing of diverse biological samples. In the absence of a R13e4 DNA substrate, the presence of ASFV infections was not detectable, despite a high amount of purified ASFV genomic DNA (2491 fM) being used (Figure 5D). Excitingly, the DSAC system applied to paper-based lateral flow strip paper was able to detect target DNA at a LOD of 83 fM (Figure 5E). We also used this platform to detect the blood sample with or without ASFV infection. They can be accurately distinguished by the DSAC system using a lateral flow strip detection platform (Figure 5F). This implies that the addition of R13e4 DNA substrate significantly improved detection the sensitivity of ASFV infections, with more than 100× better LOD of detection.

CRISPR/Dx System with a Competitor-Based DNA Substrate. During the screening of a DNA substrate with various conformations, we identified a competitor-based DNA substrate that decreases the fluorescent signals in the presence of target DNA. To assemble this competitor-based DNA substrate, we annealed two single-stranded DNA oligos to form a bicyclic substrate, CH9 (Figure 6A). The bicyclic substrate comprises two ring structures, where each ring structure was formed from self-complementary CG-rich sequences at the 5′ end and 3′ end of each DNA oligo. Single-stranded DNA in each ring structure is T-rich to enable trans-cleavage by active Cas12a. The paired region in the middle of each ring structure is composed of a crRNA sequence targeting the ASFV genomic DNA. The paired regions of these two ring structures are complementary to each other, thereby forming a double-ring structure upon annealing.

In the absence of target DNA, there was no trans-cleavage activity to cleave the T-rich ssDNA in the CH9 DNA substrate. However, inactive Cas12a can access and bind to the dsDNA region in the paired region of two ring structures, resulting in activation of trans-cleavage activity to cleave nearby probes to generate strong fluorescent signals. In the presence of target DNA, active Cas12 induced by the target DNA also trans cleaves the T-rich single-stranded DNA in the CH9 DNA substrate. The linearized bicyclic substrate bears multiple T-rich ssDNA that is susceptible to trans-cleavage by active Cas12a. The fluorescent probes used in the CRISPR/Dx system are rich in a "T" base.[4,18] Therefore, the open single-stranded DNAs in the bicyclic substrate competed with the fluorescent probes for trans-cleavage by active Cas12a. As a consequence, the fluorescent signals declined in the presence of the target DNA in this CRISPR/Dx system.

With the optimized parameter settings, we first compared this CH9-based DSAC system with the traditional CRISPR/Cas12a system (Figure 6B). In the DSAC detection approach, the fluorescent signals decline in the presence of ASFV genomic DNA, implying the ability of the CH9-based DSAC system to detect the target DNA. Conversely, no change in the relative fluorescent signal was observed with the traditional CRISPR/Cas12a system, indicating a higher sensitivity of the DSAC system than the latter approach. Next, we tested the specificity of this DSAC system (Figure 6C,D). The addition of scramble DNA would not decrease fluorescent signals, thereby confirming the specificity of our DSAC system in detecting ASFV genomic DNA. To achieve a 99.7% confidence level of the true positive rate, the relative fluorescent threshold was set at mean − 3 SD = 1.104 − 3 × 0.099 = 0.807 ≈ 0.8.[17] Using the CH9-based CRISPR/Dx system, the sample was regarded as positive or in the presence of ASFV if the

fluorescent signal relative to the negative control (DNA substrate without the target DNA) was less than 0.8.

To explore whether the CH9-based DSAC system has a dose-dependent effect, we determine the correlation between the sample load (target DNA amount) and the relative fluorescent signals. When a higher concentration of target DNA was added, the fluorescence curve declined correspondingly (Figure 6E). The results show that the CH9-based CRISPR/Dx system enabled the detection of unamplified ASFV genomic DNA at an LOD of 249 fM (Figure 6F). Importantly, the fluorescent signal was strongly inversely proportional to the sample load (Figure 6G), further supporting the specificity of this CRISPR/Dx detection system. The CH9-based CRISPR/Dx system has also been successfully applied to a lateral flow strip paper detection platform (Figure 6H). It allows for detection at an LOD of 498 fM of unamplified ASFV genomic DNA. In contrast to the nicked- and loop-based DNA substrates, the appearance of two lines (both test line and control line) in the lateral flow strip paper indicates the negative samples in the competitor-based DSAC system. The positive samples only display one line.

To maximize the detection sensitivity of the CH9-based DSAC system, several parameters, including the reaction time of CRISPR/Cas12a and concentrations of the CH9 DNA substrate, $MgCl_2$, Cas12a, and probe, were optimized (Figure S7). In contrast to nicked-based and loop-based DNA substrates, lower relative fluorescent signals indicate greater competition effects and hence better discrimination capability and detection sensitivity.

To determine the shortest reaction time for detection, DSAC was carried out at various reaction times (Figure S7A). The relative fluorescent signals reached the plateau at 20 min; therefore, 20 min of reaction time was selected for the downstream experiments. Next, we optimized the concentration of the bicyclic substrate for detection (Figure S7B). The bicyclic substrate was serially diluted to 20−200× from 3 μM of stock solution. We found that 50× dilution resulted in the greatest decline in fluorescent signals upon the addition of target DNA. Although 20× dilution also substantially decreased relative fluorescence signals in the presence of target DNA, the background signal was high. Meanwhile, 100× and 200× dilutions of bicyclic substrate exerted weak fluorescent signals, and there was almost no change to the relative fluorescent signal when target DNA was added.

The dosage of 25 mM $MgCl_2$ was also taken into consideration (Figure S7C). Although 1.5 and 3 μL resulted in the greatest decline in relative fluorescent signals, 1.5 μL of 25 mM $MgCl_2$ was selected owing to its low variability and high consistency. Next, we evaluated the impact of Cas12a concentration on DSAC detection (Figure S7D). We found that 0.25 and 0.5 μL resulted in the greatest decline in relative fluorescent efficiency in the presence of target DNA. However, 0.5 μL of Cas12a generated stronger fluorescent intensity than the 0.25 μL, which was thereby selected for further testing. The probe concentration was then tested (Figure S7E). We selected 1 μL of 10 mM probe for downstream experiments owing to its ability to detect the presence of target DNA at a minimal amount and reduced cost.

DSAC System is Applicable to Detecting Human DNA. As our DSAC system theoretically can be used to detect any DNA sequence regarding the sources, next, we extended the application of our competitor-based DSAC system to detect human DNA. Our DSAC system can be adapted for the
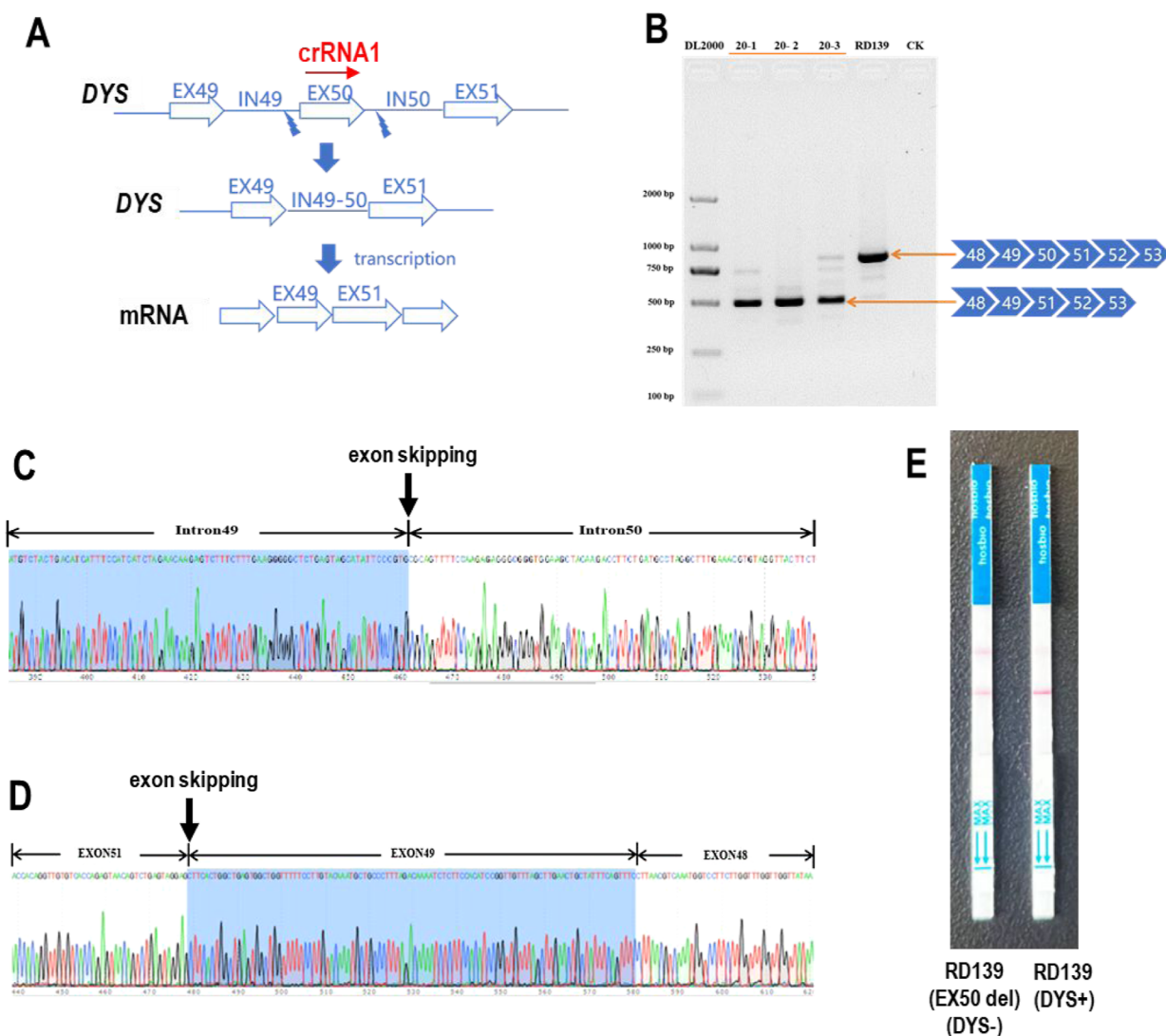
Figure 7. Detection of human DNA with a competitor-based DNA substrate. (A) crRNA1 target site on *DYS*. (B) Genomic PCR, (C) DNA sequencing, and (D) cDNA sequencing confirmation of exon-50 deletion in the *DYS* gene. (E) Lateral flow strip paper detection of exon-50 deletion in the *DYS* gene.

detection of human nucleic acids by simply providing an additional crRNA targeting the human genome. To realize such generalization, we redesign crRNA1 to target human DNA instead of ASFV genomic DNA, while the crRNA2-targeting DNA substrate remains unchanged. As an example, crRNA1 was designed to target the exon-50 of the human dystrophin gene (*DYS*). This new crRNA1 was functionally validated before being added to the competitor-based DSAC system (Figure S8).

The resulting interpretation for lateral flow strip paper detection with the competitor-based DSAC system seems unconventional, where the appearance of two lines indicates negative, while one line represents positive. It can be very useful for the detection of deletion mutations relevant to human diseases such as Duchenne muscular dystrophy (DMD). DMD is a severe type of muscular dystrophy that is caused by a deletion mutation of the exon in the dystrophin gene. RD139 cell line has a normal dystrophin gene, while the RD139 (EX50 del) cell line has a deleted exon-50 in the dystrophin gene owing to exon skipping during mRNA transcription and alternative splicing (Figure 7A). Therefore,

the RD139 (EX50 del) cell line can be regarded as a model of DMD. Genomic PCR (Figure 7B), genomic DNA sequencing (Figure 7C), and cDNA sequencing (Figure 7D) were employed to successfully verify the deletion of exon 50. Genomic DNA of RD139 and RD139 (EX50 del) were used to evaluate the performance of a competitor-based DSAC system in detecting DMD (Figure 7E). The competitor-based DSAC system allows for lateral flow strip paper detection of DMD through the observance of two lines. If there is no deletion and only the presence of the wild-type DNA, only one line appeared in the lateral flow strip paper. Therefore, the competitor-based DNA substrate CRISPR/Dx system can be potentially translated into a lateral flow strip detection platform for public use.

■ DISCUSSION

In this study, we have successfully developed two types of DSAC systems, namely, looped- and competitor-based DNA substrates, for rapid, accurate, and sensitive detection of unamplified viral nucleic acids from blood samples. To our knowledge, this is the first time annealed DNA substrates with

different conformations were used as signal enhancements in an amplification-free CRISPR/Dx system. Only three similar amplification-free CRISPR/Dx systems were reported so far; they were nonetheless different in detection principles. In a recent study, a Cas12a autocatalysis-driven positive feedback circuit (CONAN) was developed using switchable-caged guide RNA (scgRNA) with self-reporting capability for isothermally amplified detection of genomic DNA.[19] scgRNA integrated the crRNA of Cas12 and DNA probe. Although superior detection sensitivity was attained in CONAN, fabrication and screening for optimal scgRNA can be tedious and costly. Moreover, self-assembly of guide RNA released from scgRNA at constant, low temperature can be slow and inefficient.

Although a cascade Cas13a-Cas14a (casCRISPR) system developed in another recent study enabled amplification-free microRNA sensing with fM-sensitivity, the detection is long (80 min).[20] On the contrary, the detection time of our DSAC system was only 20 min. Similar to our study, two rounds of trans-cleavages were activated in their study. In their study, the presence of target miRNA first activated the trans-cleavage activity of Cas13a, which subsequently transformed the stable hairpin structure into a duplex structure with a 5′-toehold. The cleaved hairpin structure in turn activated the trans-cleavage activity of Cas14a, resulting in signal amplification. Compared to their system using a hybrid DNA-RNA hairpin structure and two Cas enzymes, only a DNA-based substrate and a Cas12a were needed in our DSAC system, thereby greatly reducing the cost and simplifying the procedures of detection.

Similar to our DSAC system, the LbuCas13−TtCsm6 system that was developed using tandem CRISPR nucleases has a detection time of 20 min[21] A chemically stabilized Csm6-activating oligonucleotide (TtCsm6 activator) serves as a bridge between the trans-cleavage of Cas13a and the RNA substrate of Csm6. In their study, TtCsm6 was first activated by LbuCas13 assembled with a crRNA. The activated TtCsm6, in turn, cleaved the fluorophore-quencher RNA reporter and generated fluorescent signals. Though the detection time of this amplification-free LbuCas13−TtCsm6 system is short and highly sensitive, the cost of detection using multiple nucleases and chemically modified activator oligonucleotide is high. In this case, our DSAC system offers the advantage of lower cost.

The LOD of our DSAC system in detecting target DNA is 83fM, which is lower than a few existing signal enhancement strategies that could achieve attomolar sensitivity.[19,21−32] These signal enhancement strategies employed nanomaterials (e.g., gold nanoparticle[28] or micromotor[32]), electrochemical and piezoelectric plate biosensors (e.g., SERS nanoprobes,[22,23] graphene field-effect transistor,[24,25,29] or surface plasmon resonance-based fiber tip[27]), or cutting-edge detection technology platforms (digital bioanalysis or droplet micro-fluidic[33,34]) for amplification-free detection of nucleic acids. However, the use of this specialized equipment or facilities has increased the detection cost and complexity in operation. Our DSAC system offers advantages in terms of detection cost and simplicity. Unlike the RNA-based detection platforms, our DSAC system used DNA-based oligonucleotides, which are much more stable, cheaper, and easier to assemble into the desired secondary structure. Our DNA substrate plays two roles: one is to serve as the substrate for trans-cleavage of active Cas12a, and the other is to trigger the trans-cleavage activity of inactive Cas12a. Theoretically, this well-validated DNA substrate can be generalized to detect any genomic loci relevant to human diseases by simply using two crRNAs: one

crRNA is targeting this ASFV template-based DNA substrate, and another crRNA is targeting the human DNA. As human DNA does not contain the ASFV DNA sequence, the DNA substrate that was used to detect ASFV nucleic acids can be applied to detect human DNA, without the need to synthesize and assemble another DNA substrate. We demonstrated that our dual-guide RNA DSAC system enabled the detection of human nucleic acids without the need to do amplification.

Although the use of competitor-based DNA substrates in the DSAC system results in opposite effects such as a decrease in the fluorescent signal in the presence of a target DNA, it can provide an alternative detection approach for specific applications such as the detection of large deletions in the human genome. For example, crRNA1 of Cas12a was designed to target the deletion region. If there was no deletion and only the presence of the wild-type DNA, a weak fluorescent signal was detected or one line in the lateral flow strip paper. In the presence of deletion, a strong fluorescent signal was observed or appeared in two lines in the lateral flow strip paper. Therefore, this DSAC system will be beneficial in these particular applications.

Although the background signal cannot be completely dismissed, a reliable discrimination between negative and positive samples was achieved through the statistical approach. For example, if the relative fluorescent signal between negative and positive samples exceeds the threshold value, the sample is regarded as positive and vice versa. The background signal issue can also be minimized through the use of a lateral flow strip paper detection approach. As we have successfully employed our CRISPR/Dx system to distinguish blood samples with and without viral DNA, this implies feasible application in field tests such as detecting low-copy pathogens.

■ CONCLUSIONS

In summary, our DSAC system provides a rapid, amplification-free CRISPR/Dx detection platform to detect viral genomic DNA with femtomolar sensitivity. The DSAC system can be applied to fluorescent-based and paper-based lateral flow strip assays, providing an alternative point-of-care diagnostic tool for the accurate and timely diagnosis of virus infections. Notably, this ASFV sequence-encoded DNA substrate can be directly used for detecting human nucleic acids simply using a dual crRNA targeting system.

■ EXPERIMENTAL SECTION

Preparation of a DNA Substrate. Oligonucleotides including primers and probes were synthesized and HPLC-purified by General Bio (Table S1). The freeze-dried powder form of primer was resuspended into 100 $\mu M/\mu L$ with 1× TE buffer (Sangon Biotech) for storage. 10 $\mu M/\mu L$ working solution was prepared by further diluting stock solution with DEPC water (Biosharp). For annealing of oligonucleotides into the desired secondary structure of loop-based DNA substrate, 10 μL of DEPC water (Biosharp), 6 μL of 10 $\mu M/\mu L$ substrate solution, and 4 μL of 5× annealing buffer (Beyotime) were mixed, and the final concentration was 3 μM. For the formation of a nicked-based DNA substrate, three different oligonucleotides with 5.33 μL of 10 $\mu M/\mu L$ each (Table S2) and 4 μL of 5× annealing buffer (Beyotime) were mixed, and the final concentration was 2.67 μM. For the formation of a competitor-based-based DNA substrate (CH9), two different oligonucleotides with 6 μL of 10 $\mu M/\mu L$ each

(Table S2), 4 μL of 5× annealing buffer (Beyotime), and 4 μL of DEPC water (Biosharp) were mixed, and the final concentration was 3 μM. The oligonucleotides were annealed at 98 °C for 1 min followed by a gradual decrease of temperature, −1 °C per minute to 25 °C, using a PCR instrument (Bio-Rad). The substrate solution was stored at 4 °C.

Plasmid Amplification and Extraction. 1 μL of EGFP ligand plasmid (1 μL) (General Bio) was transformed into DH-5α *Escherichia coli* for amplification. Endofree plasmid minikit (CWBIO) was used for plasmid extraction. The plasmid concentration was measured by a nanodrop (Thermo).

ASFV Genomic DNA Extraction. The DNA extraction kit (CWBIO) was used for viral genomic DNA extraction. All operations are performed according to the manufacturer's instructions. The copy number was determined with a ddPCR instrument (Thermo).

Swine's Blood Samples. A sample release agent (Xiamen Flygene) was used to release the ASFV particles from the blood samples. The supernatant liquid containing ASFV genomic DNA was used for the downstream experiments.

Cell Culture and Genomic DNA Extraction. Genomic DNA was extracted from HEK293, A549, RD139, and RD139 (EX50 del) using a Tissue Cell Genome DNA Rapid Extraction kit (Cook Gene). Genome DNA concentration was quantified by a nanodrop (Thermo). These cell lines were purchased from ATCC and the Guangdong Trement. The cell lines were cultured in a medium consisting of Dulbecco's modified Eagle medium (Gibco), 10% fetal bovine serum (Every Green), and 1% penicillin/streptomycin (Gibco).

Fluorescence-Based Detection of the CRISPR/Dx System. The total reaction volume was 20 μL. Unless otherwise specified, the CRISPR/Dx system consists of 12.25 μL of DEPC water (Biosharp), 2 μL of 10× HOLMES buffer (Tolobio), 1.5 μL of 25 mM MgCl$_2$ solution (Sangon Biotech), 0.25 μL of 40 U/μL RNase inhibitor (Omega Bio-Tek), 0.5 μL of CrRNA2 (T8-23-AT-crRNA-ASFV) (composited by GenePharma) targeting on ASFV DNA and activated DNA substrate, 0.5 μL of 10 μM LbCas12a Nuclease (Tolobio), and 1 μL of 10 μM probe P8a-Cas12-FAM-BHQ1 (General Bio). If the dual crRNA targeting system was used, the volume of DEPC water was 11.75 and 0.5 μL of CrRNA1 targeting on human DNA. An equal amount of CrRNA1 and CrRNA2 was added to the system. The mixtures were preincubated for about 5 min to form Cas12a−crRNA complexes. 1 μL of diluted substrate solution and 1 μL of template DNA (experimental group) or DEPC water (Biosharp) (blank group) were then added. The reaction mixtures were then incubated at 37 °C for 20 min, and real-time detection of fluorescence was performed by a fluorescence detector (Deaou-16P). The fold change (relative fluorescent signals) was defined as the ratio of the fluorescence value of the experimental group (DNA substrate with added target DNA) to the fluorescence value of the blank group (DNA substrate without added target DNA).

For the R13e4-based DSAC system, we set the threshold at mean + 3 SD = 1.018 + 3 × 0.115 = 1.363 ≈ 1.5. Fold change >1.5 was regarded as positive. Based on this threshold, 99.7% of the fold change of the negative sample is distributed within the mean + 3 SD range, and vice versa. Likewise, for the CH9-based DSAC system, the fold change threshold was set at mean

− 3 SD = 1.104 − 3 × 0.099 = 0.807 ≈ 0.8. Fold change <0.8 was regarded as positive.

Lateral Flow Strip Paper Detection of the CRISPR/Dx System. The reaction mixtures were prepared similarly to fluorescent-based detection of the CRISPR/Dx system, except for the DNA probe. Biotin-labeled probe P8b-Cas12-FAM-biotin was used instead. The reaction time and dilution factor were also different. When using the R13e4-based DSAC system, the program settings were 37 °C for 30 min, followed by 65 °C for 10 min, to terminate the reaction. When using the R13e4-based DSAC system to detect ASFV with a single CrRNA, the dilution factor of the R13e4 substrate was 50×; when detecting the human gene with the dual crRNA targeting system, the dilution factor of the R13e4 substrate was 10×. When using the CH9-based DSAC system, the program settings were 37 °C for 40 min, followed by 65 °C for 10 min, and the dilution factor of the CH9 substrate was 15×. Then, 10 μL of the reaction product was diluted with 90 μL of DEPC water (Biosharp) for lateral flow strip paper analysis. The strip (Tiosbio) was inserted into the diluted reaction products and incubated for about 1 min prior to data analysis.

ddPCR. We used a droplet digital PCR instrument (Thermo) to measure the copy number of ASFV genomic DNA. The total volume of each reaction system was 17.4 μL, including 8.7 μL QuantStudio 3D Digital PCR Master Mix v2 (ABI), 0.2 μL forward primer, 0.2 μL reverse primer, 0.2 μL probe, and 8.1 μL sample DNA. 15 μL from 17.4 μL of reaction fluid was added to the chip. 164 ng/μL ASFV genome DNA was diluted to 2 and 0.2 ng/μL, and replication was carried out. The copy number of 0.2 ng/μL solution was 1729.59 and 1748.29 copies/μL. For 2 ng/μL solution, the copy number was 18,379.77 and 19,790.03 copies/μL. The copy number of 2 ng/μL gDNA was 18,000 copies/μL, so the copy number of stock solution (164 ng/μL) of ASFV gDNA was 1,500,000 copies/μL, 2491 fM.

Validation of the Exon-50 Deletion in the *DYS* Gene. RD139 cells and RD139 cells with the *DYS* gene exon-50 deletion were obtained from Guangdong Chimee Medical Technology Co., Ltd. Genomic DNA (gDNA) and mRNA were extracted from these cells for PCR detection. 1.5% agarose gel electrophoresis was used to analyze the PCR products. In addition, the PCR products were purified and sent to Shanghai Bioengineering Co., Ltd. for sequencing.

Statistical Analysis. GraphPad Prism 9 was used to perform statistical analysis and to draw the figures. Data are presented as mean ± standard deviation (SD). Statistical comparisons were performed by using two-tailed t tests and one-way ANOVA. P values less than 0.05 were considered statistically significant with $^*p < 0.05$ and $^\#p < 0.01$.

■ ASSOCIATED CONTENT

⑤ Supporting Information

The Supporting Information is available free of charge at https://pubs.acs.org/doi/10.1021/acsomega.4c03413.

> Detection principle of nicked-based DNA substrate-mediated DSAC system, validation of ASFV crRNA functionality, structure of various nicked-based substrates and loop-based substrates, effect of the target DNA template with various base mismatches on the detection specificity of our DSAC system, absolute quantification of the copy number of ASFV genomic DNA using ddPCR, validation of ASFV infections in

swine's blood sample, optimization of the CH9-based DSAC system, validation of *DYS* crRNA functionality, oligonucleotides used in this study, and oligonucleotides used to form the desired secondary structure (PDF)

■ AUTHOR INFORMATION

Corresponding Authors

Gang Chen − *Department of Pathology, Clinical Oncology School of Fujian Medical University, Fuzhou, Fujian 350014, China;* Email: naichengang@126.com

Hongman Xue − *Pediatric Hematology Laboratory, Division of Hematology/Oncology, Department of Pediatrics, The Seventh Affiliated Hospital of Sun Yat-Sen University, Shenzhen, Guangdong 518107, China;* Email: xuehm5@mail.sysu.edu.cn

Haibao Zhu − *Department of Biology, College of Science, Shantou University, Shantou, Guangdong 515063, China;* Email: zhuhaibao@stu.edu.cn

Authors

Zhongqi Zhou − *Pediatric Hematology Laboratory, Division of Hematology/Oncology, Department of Pediatrics, The Seventh Affiliated Hospital of Sun Yat-Sen University, Shenzhen, Guangdong 518107, China*

Cia-Hin Lau − *Department of Biology, College of Science, Shantou University, Shantou, Guangdong 515063, China;* orcid.org/0000-0002-4528-0363

Jianchao Wang − *Department of Pathology, Clinical Oncology School of Fujian Medical University, Fuzhou, Fujian 350014, China*

Rui Guo − *Animal Husbandry and Veterinary Institute, Hubei Academy of Agricultural Science, Wuhan, Hubei 430064, China; Key Laboratory of Prevention and Control Agents for Animal Bacteriosis, Ministry of Agriculture, Wuhan, Hubei 430064, China*

Sheng Tong − *Department of Biomedical Engineering, University of Kentucky, Lexington, Kentucky 40506-0503, United States;* orcid.org/0000-0001-8632-7933

Jiaqi Li − *Department of Biology, College of Science, Shantou University, Shantou, Guangdong 515063, China*

Wenjiao Dong − *Department of Epidemiology and Health Statistics, School of Public Health, Guangdong Medical University, Dongguan, Guangdong 523808, China*

Zhihao Huang − *Department of Biology, College of Science, Shantou University, Shantou, Guangdong 515063, China*

Tao Wang − *Department of Biology, College of Science, Shantou University, Shantou, Guangdong 515063, China*

Xiaojun Huang − *Xiamen Fly Gene Biomedical Technology CO., LTD, Xiamen, Fujian 361000, China*

Ziqing Yu − *Department of Pathology, Clinical Oncology School of Fujian Medical University, Fuzhou, Fujian 350014, China*

Chiju Wei − *Department of Biology, College of Science, Shantou University, Shantou, Guangdong 515063, China*

Complete contact information is available at:
https://pubs.acs.org/10.1021/acsomega.4c03413

Author Contributions

○Z.Z., C.-H.L., and J.W. contributed equally. H.Z., G.C., and H.X. conceived and supervised the project. Z.Z., J.W., J.L., W.D., Z.H., T.W., X.H., and Z.Y. performed the experiments and collected and analyzed the data. R.G. is responsible for collecting African swine fever samples. H.Z., H.X., G.C., C.W., S.T., and C.-H.L. wrote and revised the manuscript. All authors read, corrected, and approved the final manuscript.

Notes

The authors declare no competing financial interest.

■ ABBREVIATIONS

ASFV, African swine fever virus; ATCC, American Type Culture Collection; Cas12a, CRISPR associated protein 12a; CONAN, Cas12a autocatalysis-driven positive feedback circuit; casCRISPR, cascade Cas13a−Cas14a; CRISPR, clustered regularly interspaced short palindromic repeats; CRISPR/Dx, CRISPR-based diagnostics; crRNA, CRISPR RNA; ddPCR, digital PCR; DEPC, diethylpyrocarbonate; DMD, Duchenne muscular dystrophy; DSAC, DNA substrate-mediated autocatalysis of CRISPR/Cas12a; dsDNA, double stranded DNA; DYS, dystrophin; EGFP, enhanced green fluorescent protein; ERBB2, erb-b2 receptor tyrosine kinase 2; HPLC, high-performance liquid chromatography; IVD, in vitro diagnostics; LOD, limit of detection; PCR, polymerase chain reaction; POCT, point-of-care testing; SD, standard deviation

■ REFERENCES

(1) Stower, H. Crispr-Based Diagnostics. *Nat. Med.* **2018**, *24*, 702.

(2) Kaminski, M. M.; Abudayyeh, O. O.; Gootenberg, J. S.; Zhang, F.; Collins, J. J. Crispr-Based Diagnostics. *Nat. Biomed. Eng.* **2021**, *5*, 643−656.

(3) Zetsche, B.; Gootenberg, J. S.; Abudayyeh, O. O.; Slaymaker, I. M.; Makarova, K. S.; Essletzbichler, P.; Volz, S. E.; Joung, J.; van der Oost, J.; Regev, A.; Koonin, E. V.; Zhang, F. Cpf1 Is a Single Rna-Guided Endonuclease of a Class 2 Crispr-Cas System. *Cell* **2015**, *163*, 759−771.

(4) Chen, J. S.; Ma, E.; Harrington, L. B.; Da Costa, M.; Tian, X.; Palefsky, J. M.; Doudna, J. A. Crispr-Cas12a Target Binding Unleashes Indiscriminate Single-Stranded Dnase Activity. *Science* **2018**, *360*, 436−439.

(5) Abudayyeh, O. O.; Gootenberg, J. S.; Essletzbichler, P.; Han, S.; Joung, J.; Belanto, J. J.; Verdine, V.; Cox, D. B. T.; Kellner, M. J.; Regev, A.; Lander, E. S.; Voytas, D. F.; Ting, A. Y.; Zhang, F. Rna Targeting with Crispr-Cas13. *Nature* **2017**, *550*, 280−284.

(6) Cox, D. B. T.; Gootenberg, J. S.; Abudayyeh, O. O.; Franklin, B.; Kellner, M. J.; Joung, J.; Zhang, F. Rna Editing with Crispr-Cas13. *Science* **2017**, *358*, 1019−1027.

(7) Feng, W.; Newbigging, A. M.; Tao, J.; Cao, Y.; Peng, H.; Le, C.; Wu, J.; Pang, B.; Li, J.; Tyrrell, D. L.; Zhang, H.; Le, X. C. Crispr Technology Incorporating Amplification Strategies: Molecular Assays for Nucleic Acids, Proteins, and Small Molecules. *Chem. Sci.* **2021**, *12*, 4683−4698.

(8) Mao, X.; Xu, M.; Luo, S.; Yang, Y.; Zhong, J.; Zhou, J.; Fan, H.; Li, X.; Chen, Z. Advancements in the Synergy of Isothermal Amplification and Crispr-Cas Technologies for Pathogen Detection. *Front. Bioeng. Biotechnol.* **2023**, *11*, 1273988.

(9) Li, H.; Xie, Y.; Chen, F.; Bai, H.; Xiu, L.; Zhou, X.; Guo, X.; Hu, Q.; Yin, K. Amplification-Free Crispr/Cas Detection Technology:

Challenges, Strategies, and Perspectives. *Chem. Soc. Rev.* **2023**, *52*, 361−382.

(10) Zhang, J.; Lv, H.; Li, L.; Chen, M.; Gu, D.; Wang, J.; Xu, Y. Recent Improvements in Crispr-Based Amplification-Free Pathogen Detection. *Front. Microbiol.* **2021**, *12*, 751408.

(11) Ji, S.; Wang, X.; Wang, Y.; Sun, Y.; Su, Y.; Lv, X.; Song, X. Advances in Cas12a-Based Amplification-Free Nucleic Acid Detection. *CRISPR J.* **2023**, *6*, 405−418.

(12) Talebian, S.; Dehghani, F.; Weiss, P. S.; Conde, J. Evolution of Crispr-Enabled Biosensors for Amplification-Free Nucleic Acid Detection. *Trends Biotechnol.* **2024**, *42*, 10−13.

(13) Shinoda, H.; Taguchi, Y.; Nakagawa, R.; Makino, A.; Okazaki, S.; Nakano, M.; Muramoto, Y.; Takahashi, C.; Takahashi, I.; Ando, J.; Noda, T.; Nureki, O.; Nishimasu, H.; Watanabe, R. Amplification-Free Rna Detection with Crispr-Cas13. *Commun. Biol.* **2021**, *4*, 476.

(14) Qian, S.; Chen, Y.; Xu, X.; Peng, C.; Wang, X.; Wu, H.; Liu, Y.; Zhong, X.; Xu, J.; Wu, J. Advances in Amplification-Free Detection of Nucleic Acid: Crispr/Cas System as a Powerful Tool. *Anal. Biochem.* **2022**, *643*, 114593.

(15) Liu, P. F.; Zhao, K. R.; Liu, Z. J.; Wang, L.; Ye, S. Y.; Liang, G. X. Cas12a-Based Electrochemiluminescence Biosensor for Target Amplification-Free DNA Detection. *Biosens. Bioelectron.* **2021**, *176*, 112954.

(16) Wang, H.; Su, A.; Bao, C.; Liang, C.; Xu, W.; Chang, J.; Xu, S. A Crispr/Cas12a-Sers Platform for Amplification-Free Detection of African Swine Fever Virus Genes. *Talanta* **2024**, *267*, 125225.

(17) Abdool, A.; Donahue, A. C.; Wohlgemuth, J. G.; Yeh, C. H. Detection, Analysis and Clinical Validation of Chromosomal Aberrations by Multiplex Ligation-Dependent Probe Amplification in Chronic Leukemia. *PLoS One* **2010**, *5*, No. e15407.

(18) Nguyen, L. T.; Smith, B. M.; Jain, P. K. Enhancement of Trans-Cleavage Activity of Cas12a with Engineered Crrna Enables Amplified Nucleic Acid Detection. *Nat. Commun.* **2020**, *11*, 4906.

(19) Shi, K.; Xie, S.; Tian, R.; Wang, S.; Lu, Q.; Gao, D.; Lei, C.; Zhu, H.; Nie, Z. A Crispr-Cas Autocatalysis-Driven Feedback Amplification Network for Supersensitive DNA Diagnostics. *Sci. Adv.* **2021**, *7*, No. eabc7802.

(20) Sha, Y.; Huang, R.; Huang, M.; Yue, H.; Shan, Y.; Hu, J.; Xing, D. Cascade Crispr/Cas Enables Amplification-Free Microrna Sensing with Fm-Sensitivity and Single-Base-Specificity. *Chem. Commun.* **2021**, *57*, 247−250.

(21) Liu, T. Y.; Knott, G. J.; Smock, D. C. J.; Desmarais, J. J.; Son, S.; Bhuiya, A.; Jakhanwal, S.; Prywes, N.; Agrawal, S.; Diaz de Leon Derby, M.; Switz, N. A.; Armstrong, M.; Harris, A. R.; Charles, E. J.; Thornton, B. W.; Fozouni, P.; Shu, J.; Stephens, S. I.; Kumar, G. R.; Zhao, C.; Mok, A.; Iavarone, A. T.; Escajeda, A. M.; McIntosh, R.; Kim, S.; Dugan, E. J.; Hamilton, J. R.; Lin-Shiao, E.; Stahl, E. C.; Tsuchida, C. A.; Moehle, E. A.; Giannikopoulos, P.; McElroy, M.; McDevitt, S.; Zur, A.; et al. Accelerated Rna Detection Using Tandem Crispr Nucleases. *Nat. Chem. Biol.* **2021**, *17*, 982−988.

(22) Yin, B.; Zhang, Q.; Xia, X.; Li, C.; Ho, W. K. H.; Yan, J.; Huang, Y.; Wu, H.; Wang, P.; Yi, C.; Hao, J.; Wang, J.; Chen, H.; Wong, S. H. D.; Yang, M. A Crispr-Cas12a Integrated Sers Nanoplatform with Chimeric DNA/Rna Hairpin Guide for Ultrasensitive Nucleic Acid Detection. *Theranostics* **2022**, *12*, 5914−5930.

(23) Choi, J. H.; Shin, M.; Yang, L.; Conley, B.; Yoon, J.; Lee, S. N.; Lee, K. B.; Choi, J. W. Clustered Regularly Interspaced Short Palindromic Repeats-Mediated Amplification-Free Detection of Viral Dnas Using Surface-Enhanced Raman Spectroscopy-Active Nano-array. *ACS Nano* **2021**, *15*, 13475−13485.

(24) Wang, H.; Sun, Y.; Zhou, Y.; Liu, Y.; Chen, S.; Sun, W.; Zhang, Z.; Guo, J.; Yang, C.; Li, Z.; Chen, L. Unamplified System for Sensitive and Typing Detection of Asfv by the Cascade Platform That Crispr-Cas12a Combined with Graphene Field-Effect Transistor. *Biosens. Bioelectron.* **2023**, *240*, 115637.

(25) Weng, Z.; You, Z.; Li, H.; Wu, G.; Song, Y.; Sun, H.; Fradlin, A.; Neal-Harris, C.; Lin, M.; Gao, X.; Zhang, Y. Crispr-Cas12a Biosensor Array for Ultrasensitive Detection of Unamplified DNA

with Single-Nucleotide Polymorphic Discrimination. *ACS Sens.* **2023**, *8*, 1489−1499.

(26) Yue, H.; Shu, B.; Tian, T.; Xiong, E.; Huang, M.; Zhu, D.; Sun, J.; Liu, Q.; Wang, S.; Li, Y.; Zhou, X. Droplet Cas12a Assay Enables DNA Quantification from Unamplified Samples at the Single-Molecule Level. *Nano Lett.* **2021**, *21*, 4643−4653.

(27) Chen, Y.; Chen, Z.; Li, T.; Qiu, M.; Zhang, J.; Wang, Y.; Yuan, W.; Ho, A. H.; Al-Hartomy, O.; Wageh, S.; Al-Sehemi, A. G.; Shi, X.; Li, J.; Xie, Z.; Xuejin, L.; Zhang, H. Ultrasensitive and Specific Clustered Regularly Interspaced Short Palindromic Repeats Empowered a Plasmonic Fiber Tip System for Amplification-Free Monkeypox Virus Detection and Genotyping. *ACS Nano* **2023**, *17*, 12903−12914.

(28) Zhou, J.; Hu, J.; Liu, R.; Wang, C.; Lv, Y. Dual-Amplified Crispr-Cas12a Bioassay for Hiv-Related Nucleic Acids. *Chem. Commun.* **2022**, *58*, 4247−4250.

(29) Li, H.; Yang, J.; Wu, G.; Weng, Z.; Song, Y.; Zhang, Y.; Vanegas, J. A.; Avery, L.; Gao, Z.; Sun, H.; Chen, Y.; Dieckhaus, K. D.; Gao, X.; Zhang, Y. Amplification-Free Detection of Sars-Cov-2 and Respiratory Syncytial Virus Using Crispr Cas13a and Graphene Field-Effect Transistors. *Angew. Chem., Int. Ed.* **2022**, *61*, No. e202203826.

(30) Li, J.; Tang, L.; Li, T.; Li, K.; Zhang, Y.; Ni, W.; Xiao, M. M.; Zhao, Y.; Zhang, Z. Y.; Zhang, G. J. Tandem Cas13a/Crrna-Mediated Crispr-Fet Biosensor: A One-for-All Check Station for Virus without Amplification. *ACS Sens.* **2022**, *7*, 2680−2690.

(31) Zhang, Y.; Chen, Y.; Zhang, Q.; Liu, Y.; Zhang, X. An Am-Level Sensitive Cascade Crispr-Dx System (Ascas) for Rapid Detection of Rna without Pre-Amplification. *Biosens. Bioelectron.* **2023**, *230*, 115248.

(32) Chen, D.; Liang, Y.; Wang, H.; Wang, H.; Su, F.; Zhang, P.; Wang, S.; Liu, W.; Li, Z. Crispr-Cas-Driven Single Micromotor (Cas-Dsm) Enables Direct Detection of Nucleic Acid Biomarkers at the Single-Molecule Level. *Anal. Chem.* **2023**, *95*, 5729−5737.

(33) Iida, T.; Shinoda, H.; Watanabe, R. Satori: Amplification-Free Digital Rna Detection Method for the Diagnosis of Viral Infections. *Biophys. Physicobiol.* **2023**, *20*, No. e200031.

(34) Wang, H.; Wang, S.; Wang, H.; Tang, F.; Chen, D.; Liang, Y.; Li, Z. Amplification-Free Detection of Telomerase Activity at the Single-Cell Level Via Cas12a-Lighting-up Single Microbeads (Cas12a-Lsmbs). *Lab Chip* **2023**, *23*, 4674−4679.